

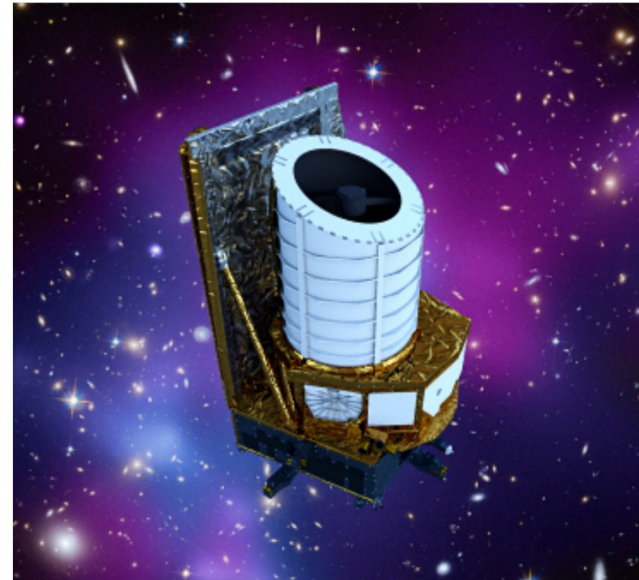


Agenzia Spaziale Italiana



The Status of the Euclid Mission

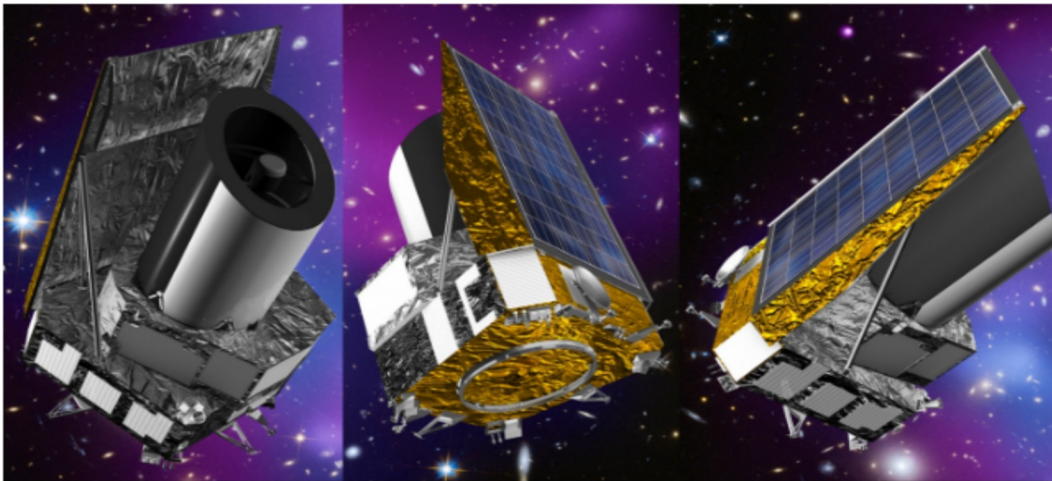
Marco Scodeggio
INAF IASF-Milano



The Euclid mission in one sentence



Euclid and the origin of the accelerating universe



Artist views of the Euclid Satellite - © ESA

Euclid is an [ESA](#) medium class astronomy and astrophysics space mission. Euclid was selected by ESA in October 2011 (see the [Euclid ESA page](#)). Its launch is planned for 2022. In June 2012 ESA officially selected the “[Euclid Consortium](#)” as the single team having the scientific responsibility of the mission, the data production and of the scientific instruments.

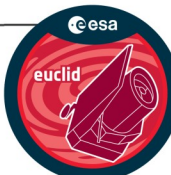
The Euclid mission aims at understanding why the expansion of the Universe is accelerating and what is the nature of the source responsible for this acceleration which physicists refer to as dark energy. Dark energy represents around 75% of the energy content of the Universe today, and together with dark matter it dominates the Universes' matter-energy content. Both are mysterious and of unknown nature but control the past, present and future evolution of Universe.



[The Euclid Community](#)

[Contacts](#)

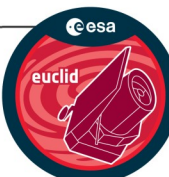
[Euclid Consortium Code of Conduct](#)



Why all this effort ??



- Cosmology in the '80s and in the '90s had a problem
- A Universe composed of 25% matter and 75% dark matter
- Then things got considerably worse at the dawn of the new millennium
- A Universe composed of 5% matter, 25% dark matter, and 70% dark energy
- Is it possible to understand a little bit better what is going on ??



The birth of the Dark Matter concept



Die Rotverschiebung von extragalaktischen Nebeln

von F. Zwicky.

(16. II. 33.)

Inhaltsangabe. Diese Arbeit gibt eine Darstellung der wesentlichsten Merkmale extragalaktischer Nebel, sowie der Methoden, welche zur Erforschung derselben gedient haben. Insbesondere wird die sog. Rotverschiebung extragalaktischer Nebel eingehend diskutiert. Verschiedene Theorien, welche zur Erklärung dieses wichtigen Phänomens aufgestellt worden sind, werden kurz besprochen. Schliesslich wird angedeutet, inwiefern die Rotverschiebung für das Studium der durchdringenden Strahlung von Wichtigkeit zu werden verspricht.

§ 1. Einleitung.

Es ist schon seit langer Zeit bekannt, dass es im Weltraum gewisse Objekte gibt, welche, wenn mit kleinen Teleskopen beobachtet, als stark verschwommene, selbstleuchtende Flecke erscheinen. Diese Objekte besitzen verschiedenartige Strukturen. Oft sind sie kugelförmig, oft elliptisch, und viele unter ihnen haben ein spiralartiges Aussehen, weshalb man sie gelegentlich als Spiralnebel bezeichnet. Dank des enormen Auflösungsvermögens der modernen Riesenteleskope gelang es, festzustellen, dass diese Nebel ausserhalb der Grenzen unseres eigenen Milchstrassensystems liegen. Aufnahmen, die mit dem Hundert-Zoll-Teleskop auf dem Mt. Wilson gemacht worden sind, offenbaren, dass diese Nebel Sternsysteme sind, ähnlich unserem eigenen Milchstrassensystem.

Fritz Zwicky 1933
Helvetica Physica Acta

Galaxies are galaxies since
Hubble's M31 work in 1924

Hubble Law in 1929

Rotverschiebung extragalaktischer Nebel.

Scheinbare Geschwindigkeiten im Comahaufen.

$v = 8500$ km/sec	6900 km/sec
7900	6700
7600	6600
7000	5100 (?)

ist möglich, dass der letzte Wert von 5100 km/sec einem sog. dnebel (field nebula) entspricht, welcher nicht dem Comasystem gehört, sondern nur in dasselbe sich projiziert. Die Wahrscheinlichkeit für diese Annahme ist allerdings nicht sehr gross ($1/16$). Auch wenn wir diesen Nebel weglassen, bleiben die Variationen im Comasystem immer noch sehr gross. Es ist in diesem Zusammenhang von Interesse, daran zu erinnern, dass die mittlere Dichte im Comahaufen die grösste bis jetzt beobachtete ist.

The birth of the Dark Matter concept



§ 5. Bemerkungen zur Streuung der Geschwindigkeiten im Coma-Nebelhaufen.

Wie aus der Zusammenstellung in § 3 hervorgeht, existieren im Comahaufen scheinbare Geschwindigkeitsunterschiede von mindestens 1500 bis 2000 km/sec. Im Zusammenhang mit dieser enormen Streuung der Geschwindigkeiten kann man folgende Überlegungen anstellen.

1. Setzt man voraus, dass das Comasystem mechanisch einen stationären Zustand erreicht hat, so folgt aus dem Virialsatz

$$\bar{\epsilon}_k = -\frac{1}{2} \bar{\epsilon}_p, \quad (4)$$

wobei $\bar{\epsilon}_k$ und $\bar{\epsilon}_p$ mittlere kinetische und potentielle Energien, z. B. der Masseneinheit im System bedeuten. Zum Zwecke der Abschätzung nehmen wir an, dass die Materie im Haufen gleichförmig über den Raum verteilt ist. Der Haufen besitzt einen Radius R von ca. einer Million Lichtjahren (gleich 10^{24} cm) und enthält 800 individuelle Nebel von je einer Masse entsprechend 10^9 Sonnenmassen. Die Gesamtmasse M des Systems ist deshalb

$$M \sim 800 \times 10^9 \times 2 \times 10^{33} = 1.6 \times 10^{45} \text{ gr.} \quad (5)$$

Daraus folgt für die totale potentielle Energie Ω :

$$\Omega = -\frac{3}{5} \Gamma \frac{M^2}{R} \quad (6)$$

Γ = Gravitationskonstante

oder

$$\bar{\epsilon}_p = \Omega/M \sim -64 \times 10^{12} \text{ cm}^2 \text{ sek}^{-2} \quad (7)$$

und weiter

$$\begin{aligned} \bar{\epsilon}_k &= \bar{v}^2/2 = -\bar{\epsilon}_p/2 = 32 \times 10^{12} \text{ cm}^2 \text{ sek}^{-2} \\ (\bar{v}^2)^{1/2} &= 80 \text{ km/sec.} \end{aligned} \quad (8)$$

Rotverschiebung extragalaktischer Nebel.

125

Um, wie beobachtet, einen mittleren Dopplereffekt von 1000 km/sec oder mehr zu erhalten, müsste also die mittlere Dichte im Comasystem mindestens 400 mal grösser sein als die auf Grund von Beobachtungen an leuchtender Materie abgeleitete¹⁾). Falls sich dies bewahrheiten sollte, würde sich also das überraschende Resultat ergeben, dass dunkle Materie in sehr viel grösserer Dichte vorhanden ist als leuchtende Materie.

2. Man kann auch annehmen, dass das Comasystem sich nicht im stationären Gleichgewicht befindet, sondern dass die ganze verfügbare potentielle Energie als kinetische Energie erscheint. Es wäre dann

$$\bar{\epsilon}_k = -\bar{\epsilon}_p. \quad (9)$$

Man kann also durch diese Annahme gegenüber 1. nur einen Faktor 2 einsparen, und die Notwendigkeit einer enorm grossen Dichte dunkler Materie bleibt bestehen.

The birth of the Dark Matter concept



§ 5. Bemerkungen zur Streuung der Geschwindigkeiten im Coma-Nebelhaufen.

Wie aus der Zusammenstellung in § 3 hervorgeht, existieren im Comahaufen scheinbare Geschwindigkeitsunterschiede von mindestens 1500 bis 2000 km/sec. Im Zusammenhang mit dieser enormen Streuung der Geschwindigkeiten kann man folgende Überlegungen anstellen.

1. Setzt man voraus, dass das Comasystem mechanisch einen stationären Zustand erreicht hat, so folgt aus dem Virialsatz

$$\bar{\epsilon}_k = -\frac{1}{2} \bar{\epsilon}_p, \quad (4)$$

wobei $\bar{\epsilon}_k$ und $\bar{\epsilon}_p$ mittlere kinetische und potentielle Energien, z. B. der Masseneinheit im System bedeuten. Zum Zwecke der Abschätzung nehmen wir an, dass die Materie im Haufen gleichförmig über den Raum verteilt ist. Der Haufen besitzt einen Radius R von ca. einer Million Lichtjahren (gleich 10^{24} cm) und enthält 800 individuelle Nebel von je einer Masse entsprechend 10^9 Sonnenmassen. Die Gesamtmasse M des Systems ist deshalb

$$M \sim 800 \times 10^9 \times 2 \times 10^{33} = 1.6 \times 10^{45} \text{ gr.} \quad (5)$$

Daraus folgt für die totale potentielle Energie Ω :

$$\Omega = -\frac{3}{5} \Gamma \frac{M^2}{R} \quad (6)$$

Γ = Gravitationskonstante

oder

$$\bar{\epsilon}_p = \Omega/M \sim -64 \times 10^{12} \text{ cm}^2 \text{ sek}^{-2} \quad (7)$$

und weiter

von Beobachtungen an leuchtender Materie abgeleitete¹). Falls sich dies bewahrheiten sollte, würde sich also das überraschende Resultat ergeben, dass dunkle Materie in sehr viel grösserer Dichte vorhanden ist als leuchtende Materie.

Rotverschiebung extragalaktischer Nebel.

125

Um, wie beobachtet, einen mittleren Dopplereffekt von 1000 km/sec oder mehr zu erhalten, müsste also die mittlere Dichte im Comasystem mindestens 400 mal grösser sein als die auf Grund von Beobachtungen an leuchtender Materie abgeleitete¹). Falls sich dies bewahrheiten sollte, würde sich also das überraschende Resultat ergeben, dass dunkle Materie in sehr viel grösserer Dichte vorhanden ist als leuchtende Materie.

2. Man kann auch annehmen, dass das Comasystem sich nicht im stationären Gleichgewicht befindet, sondern dass die Energie er-

(9)

nur einen
m grossen

Dark Matter takes center stage

THE ASTROPHYSICAL JOURNAL, 201:327–346, 1975 October 15

© 1975. The American Astronomical Society. All rights reserved. Printed in U.S.A.

THE ROTATION CURVE AND GEOMETRY OF M31 AT LARGE GALACTOCENTRIC DISTANCES

MORTON S. ROBERTS

National Radio Astronomy Observatory,* Green Bank, West Virginia
AND

ROBERT N. WHITEHURST

Department of Physics and Astronomy, The University of Alabama
Received 1975 February 7

ABSTRACT

New 21-cm observations of the southern end of M31 indicate (1) that the plane of H I is bent away from the conventional plane by up to ~ 5 kpc and (2) that the rotational velocity is essentially constant over the outer 10 kpc, i.e., from 20 to 30 kpc radius. The latter implies a mass that increases linearly with R over this range and a mass-to-luminosity ratio of $\gtrsim 200$ for this outer region. At 30 kpc the surface density is $\sim 50 M_{\odot} pc^{-2}$. Dwarf M stars, the most common type of star in the solar vicinity, of number density of a few tenths pc^{-3} are adequate to explain the required mass and the mass-to-luminosity ratio. At these distances H I is ~ 1 percent of the total mass.

Subject headings: galaxies, individual — galaxies, motions in — galaxies, stellar content of — 21-cm radiation

M31 and a Brief History of Dark Matter

287

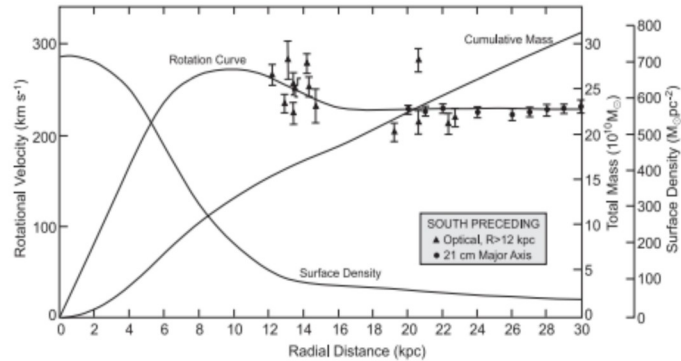


Figure 2. A smoothed rotation curve of M31 (Roberts and Whitehurst 1975). The filled triangles are based on optical observations (Rubin and Ford 1970). The filled circles are from 300 foot telescope H I measurements extending to 150'.

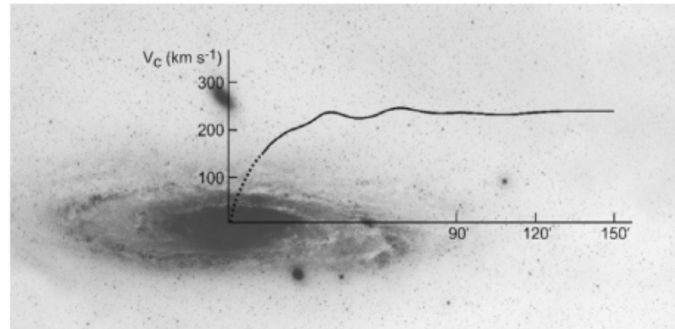


Figure 3. The rotation curve of Figure 2 superposed on an image of M31.

Dark Matter takes center stage

THE ASTROPHYSICAL JOURNAL, 225:L107-L111, 1978 November 1
© 1978. The American Astronomical Society. All rights reserved. Printed in U.S.A.



EXTENDED ROTATION CURVES OF HIGH-LUMINOSITY SPIRAL GALAXIES. IV. SYSTEMATIC DYNAMICAL PROPERTIES, Sa→Sc

VERA C. RUBIN,*† W. KENT FORD, JR.,* AND NORBERT THONNARD

Department of Terrestrial Magnetism, Carnegie Institution of Washington

Received 1978 June 7; accepted 1978 July 18

ABSTRACT

For a sample of 10 high-luminosity spiral galaxies, Sa through Sc, we have obtained accurate rotation curves which extend to about 80% of the de Vaucouleurs radii. For this sample: (1) All rotation curves are approximately flat, to distances as great as $r = 50$ kpc. Secondary velocity undulations indicate rotational velocities lower by about 20 km s^{-1} on the inner edges than on the outer edges of spiral features. (2) V_{\max} is correlated with Hubble type, and total mass M is a function of both V_{\max} and radius. At equal radii, $M(\text{Sa}) > M(\text{Sc})$. Hence, surface mass density decreases systematically along the Hubble sequence. (3) V_{\max} is not correlated with luminosity or with radius. Galaxies with similar V_{\max} have radii and luminosities which differ by factors of 2 and 3. This implies a large intrinsic scatter in the Tully-Fisher relation. (4) Masses are a few times $10^{11} M_{\odot}$ out to the de Vaucouleurs radius, and some masses approach $10^{12} M_{\odot}$ out to the Holmberg radius. M/L_B ratios are low, near 3.5. There is a weak suggestion that M/L_B is higher for early-type galaxies. While this is contrary to the accepted result of Roberts, masses for early-type galaxies are systematically low in his sample, due to an extrapolation procedure based on falling rotation curves.

Subject headings: galaxies: individual — galaxies: internal motions — galaxies: structure

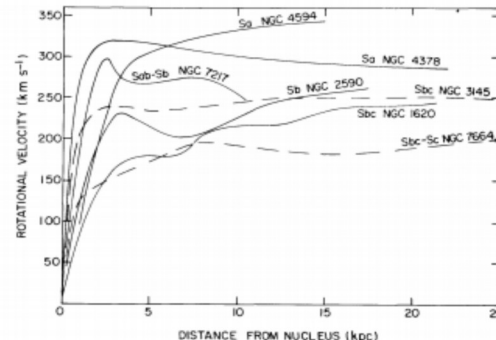


FIG. 3.—Rotational velocities for seven galaxies, as a function of distance from nucleus. Curves have been smoothed to remove velocity undulations across arms and small differences between major-axis velocities on each side of nucleus. Early-type galaxies consistently have higher peak velocities than later types.

Dark Matter takes center stage

Ann. Rev. Astron. Astrophys. 1979. 17:135–87
Copyright © 1979 by Annual Reviews Inc. All rights reserved

MASSES AND MASS-TO-LIGHT RATIOS OF GALAXIES¹ *2148

S. M. Faber²

Lick Observatory, Board of Studies in Astronomy and Astrophysics,
University of California, Santa Cruz, California 95064

J. S. Gallagher

Department of Astronomy, University of Illinois, Urbana, Illinois 61801

1 INTRODUCTION

Is there more to a galaxy than meets the eye (or can be seen on a photograph)? Many decades ago, Zwicky (1933) and Smith (1936) showed that if the Virgo cluster of galaxies is bound, the total mass must considerably exceed the sum of the masses of the individual member galaxies; i.e. there appeared to be “missing mass” in the cluster. As more data became available, the discrepancy persisted between masses of individual galaxies determined from optical rotation curves and the larger average galaxy mass needed to bind groups and clusters (e.g. Neyman, Page & Scott 1961).

Recently, however, new information has pointed toward larger total masses for individual galaxies, thus decreasing the traditional discrepancy between various methods of mass measurement. Arguing that thin, self-gravitating stellar disks are unstable against bar-like modes, Ostriker & Peebles (1973) suggested that the disks of normal spiral galaxies must be imbedded in optically undetected, stabilizing massive halos. Ostriker, Peebles & Yahil (1974) and Einasto, Kaasik & Saar (1974) collected observational evidence in support of the existence of such halos (although Burbidge 1975 used similar data to reach the opposite conclusion). At nearly the same time, high-resolution 21-cm observations of nearby galaxies were showing that H I often extends well beyond the optical

8 CODA

After reviewing all the evidence, it is our opinion that the case for invisible mass in the Universe is very strong and getting stronger. Particularly encouraging is the fact that the mass-to-light ratio for binaries agrees so well with that for small groups. Furthermore, our detailed knowledge of the mass distribution of the Milky Way and Local Group is reassuringly consistent with the mean properties of galaxies and groups elsewhere. In sum, although such questions as observational errors and membership probabilities are not yet completely resolved, we think it likely that the discovery of invisible matter will endure as one of the major conclusions of modern astronomy.

In addition to the dynamical evidence, there are other indirect indications of dark material in galaxies. The most important of these are the stability analyses of cold, self-gravitating axisymmetric disks (e.g. Ostriker & Peebles 1973, Hohl 1976, Miller 1978), which show them to be susceptible to bar-formation if not stabilized by a hot dynamical component. This hot component may or may not be related to massive envelopes.

Although present data give us little information on the shape of massive envelopes, further study of the outermost hydrogen in spirals may tell us more about this question. For example, the apparent lifetime of warps in many spirals poses severe theoretical difficulties as long as it is assumed that disks are self-gravitating (e.g. Binney 1978, Bosma 1978). This problem would not arise if the warps existed within the potential of a nearly spherical massive envelope. The precession of the warp due to the torque of the disk would then be much smaller, and the warp would be very long-lived. Alternatively, Binney (1978) has suggested that a warp might actually be driven by a triaxial dark halo. Finally, z-motions of H I far from the nucleus can be used to measure the space density of matter in the plane and thus to set limits on the flattening of the envelope.

Despite the general lack of observational evidence on the shapes of



The re-birth of Dark Energy

- November 1915, Einstein presents GR

$$R_{\mu\nu} - \frac{1}{2} R g_{\mu\nu} = 8\pi G T_{\mu\nu}$$

- 1917, Einstein introduces the Cosmological Constant, to allow for a static Universe

$$R_{\mu\nu} - \frac{1}{2} R g_{\mu\nu} + \Lambda g_{\mu\nu} = 8\pi G T_{\mu\nu}$$

- 1922, Friedmann proposes a solution of GR equations which describes an expanding universe that contains moving matter
- So the Cosmological Constant gets taken out of GR...
- But in 1998 it makes an unexpected come-back !!

Dark Energy and the accelerated expansion of the Universe

THE ASTRONOMICAL JOURNAL, 116:1009–1038, 1998 September
© 1998. The American Astronomical Society. All rights reserved. Printed in U.S.A.



OBSERVATIONAL EVIDENCE FROM SUPERNOVAE FOR AN ACCELERATING UNIVERSE AND A COSMOLOGICAL CONSTANT

ADAM G. RIESS,¹ ALEXEI V. FILIPPENKO,¹ PETER CHALLIS,² ALEJANDRO CLOCCHIATTI,³ ALAN DIERCKS,⁴
PETER M. GARNAVICH,² RON L. GILLILAND,⁵ CRAIG J. HOGAN,⁴ SAURABH JHA,² ROBERT P. KIRSHNER,²
B. LEIBUNDGUT,⁶ M. M. PHILLIPS,⁷ DAVID REISS,⁴ BRIAN P. SCHMIDT,^{8,9} ROBERT A. SCHOMMER,⁷
R. CHRIS SMITH,^{7,10} J. SPYROMILIO,⁶ CHRISTOPHER STUBBS,⁴
NICHOLAS B. SUNTZEFF,⁷ AND JOHN TONRY¹¹

Received 1998 March 13; revised 1998 May 6

ABSTRACT

We present spectral and photometric observations of 10 Type Ia supernovae (SNe Ia) in the redshift range $0.16 \leq z \leq 0.62$. The luminosity distances of these objects are determined by methods that employ relations between SN Ia luminosity and light curve shape. Combined with previous data from our High- z Supernova Search Team and recent results by Riess et al., this expanded set of 16 high-redshift supernovae and a set of 34 nearby supernovae are used to place constraints on the following cosmological parameters: the Hubble constant (H_0), the mass density (Ω_M), the cosmological constant (i.e., the vacuum energy density, Ω_Λ), the deceleration parameter (q_0), and the dynamical age of the universe (t_0). The distances of the high-redshift SNe Ia are, on average, 10%–15% farther than expected in a low mass density ($\Omega_M = 0.2$) universe without a cosmological constant. Different light curve fitting methods, SN Ia subsamples, and prior constraints unanimously favor eternally expanding models with positive cosmological constant (i.e., $\Omega_\Lambda > 0$) and a current acceleration of the expansion (i.e., $q_0 < 0$). With no prior constraint on mass density other than $\Omega_M \geq 0$, the spectroscopically confirmed SNe Ia are statistically consistent with $q_0 < 0$ at the 2.8σ and 3.9σ confidence levels, and with $\Omega_\Lambda > 0$ at the 3.0σ and 4.0σ confidence levels, for two different fitting methods, respectively. Fixing a “minimal” mass density, $\Omega_M = 0.2$, results in the weakest detection, $\Omega_\Lambda > 0$ at the 3.0σ confidence level from one of the two methods. For a flat universe prior ($\Omega_M + \Omega_\Lambda = 1$), the spectroscopically confirmed SNe Ia require $\Omega_\Lambda > 0$ at 7σ and 9σ formal statistical significance for the two different fitting methods. A universe closed by ordinary matter (i.e., $\Omega_M = 1$) is formally ruled out at the 7σ to 8σ confidence level for the two different fitting methods. We estimate the dynamical age of the universe to be 14.2 ± 1.7 Gyr including systematic uncertainties in the current Cepheid distance scale. We estimate the likely effect of several sources of systematic error, including progenitor and metallicity evolution, extinction, sample selection bias, local perturbations in the expansion rate, gravitational lensing, and sample contamination. Presently, none of these effects appear to reconcile the data with $\Omega_\Lambda = 0$ and $q_0 \geq 0$.

Key words: cosmology: observations — supernovae: general

Dark Energy and the accelerated expansion of the Universe



1022

RIESS ET AL.

Vol. 116

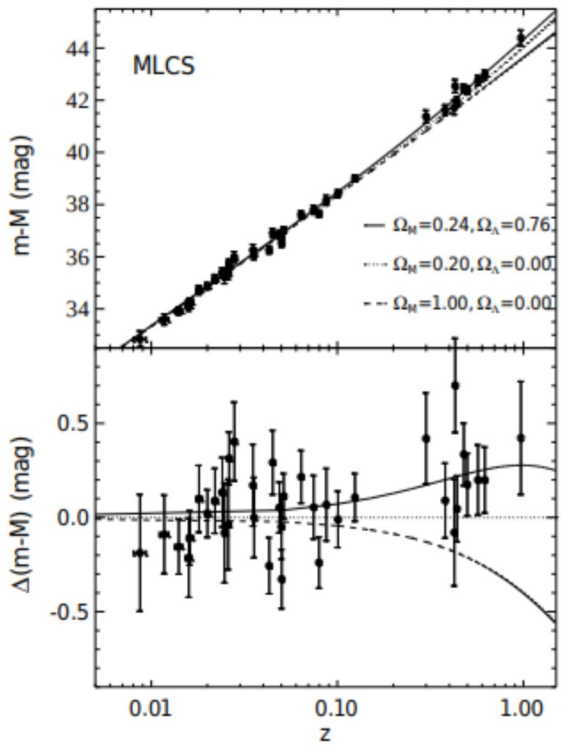


FIG. 4.—MLCS SNe Ia Hubble diagram. The upper panel shows the Hubble diagram for the low-redshift and high-redshift SNe Ia samples with distances measured from the MLCS method (Riess et al. 1995, 1996a; Appendix of this paper). Overplotted are three cosmologies: “low” and “high” Ω_M with $\Omega_A = 0$ and the best fit for a flat cosmology, $\Omega_M = 0.24$, $\Omega_A = 0.76$. The bottom panel shows the difference between data and models with $\Omega_M = 0.20$, $\Omega_A = 0$. The open symbol is SN 1997ck ($z = 0.97$), which lacks spectroscopic classification and a color measurement. The average difference between the data and the $\Omega_M = 0.20$, $\Omega_A = 0$ prediction is 0.25 mag.

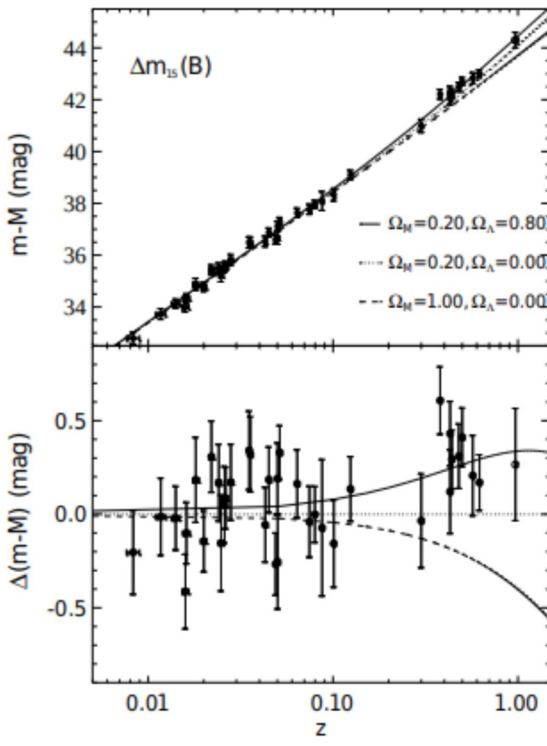


FIG. 5.— $\Delta m_{15}(B)$ SN Ia Hubble diagram. The upper panel shows the Hubble diagram for the low-redshift and high-redshift SNe Ia samples with distances measured from the template-fitting method parameterized by $\Delta m_{15}(B)$ (Hamuy et al. 1995, 1996d). Overplotted are three cosmologies: “low” and “high” Ω_M with $\Omega_A = 0$ and the best fit for a flat cosmology, $\Omega_M = 0.20$, $\Omega_A = 0.80$. The bottom panel shows the difference between data and models from the $\Omega_M = 0.20$, $\Omega_A = 0$ prediction. The open symbol is SN 1997ck ($z = 0.97$), which lacks spectroscopic classification and a color measurement. The average difference between the data and the $\Omega_M = 0.20$, $\Omega_A = 0$ prediction is 0.28 mag.

Dark Energy and the accelerated expansion of the Universe

THE ASTROPHYSICAL JOURNAL, 517: 565–586, 1999 June 1
© 1999. The American Astronomical Society. All rights reserved. Printed in U.S.A.



MEASUREMENTS OF Ω AND Λ FROM 42 HIGH-REDSHIFT SUPERNOVAE

S. PERLMUTTER,¹ G. ALDERING, G. GOLDHABER,¹ R. A. KNOP, P. NUGENT, P. G. CASTRO,² S. DEUSTUA, S. FABBRO,³
A. GOOBAR,⁴ D. E. GROOM, I. M. HOOK,⁵ A. G. KIM,^{1,6} M. Y. KIM, J. C. LEE,⁷ N. J. NUNES,² R. PAIN,³
C. R. PENNYPACKER,⁸ AND R. QUIMBY

Institute for Nuclear and Particle Astrophysics, E.O. Lawrence Berkeley National Laboratory, Berkeley, CA 94720

C. LIDMAN

European Southern Observatory, La Silla, Chile

R. S. ELLIS, M. IRWIN, AND R. G. McMAHON

Institute of Astronomy, Cambridge, England, UK

P. RUIZ-LAPUENTE

Department of Astronomy, University of Barcelona, Barcelona, Spain

N. WALTON

Isaac Newton Group, La Palma, Spain

B. SCHAEFER

Department of Astronomy, Yale University, New Haven, CT

B. J. BOYLE

Anglo-Australian Observatory, Sydney, Australia

A. V FILIPPENKO AND T. MATHESON

Department of Astronomy, University of California, Berkeley, CA

A. S. FRUCHTER AND N. PANAGIA⁹

Space Telescope Science Institute, Baltimore, MD

H. J. M. NEWBERG

Fermi National Laboratory, Batavia, IL

AND

W. J. COUCH

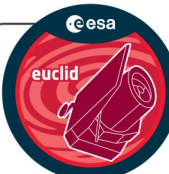
University of New South Wales, Sydney, Australia

(THE SUPERNOVA COSMOLOGY PROJECT)

Received 1998 September 8; accepted 1998 December 17

ABSTRACT

We report measurements of the mass density, Ω_M , and cosmological-constant energy density, Ω_Λ , of the universe based on the analysis of 42 type Ia supernovae discovered by the Supernova Cosmology Project. The magnitude-redshift data for these supernovae, at redshifts between 0.18 and 0.83, are fitted jointly with a set of supernovae from the Calán/Tololo Supernova Survey, at redshifts below 0.1, to yield values for the cosmological parameters. All supernova peak magnitudes are standardized using a SN Ia light-curve width-luminosity relation. The measurement yields a joint probability distribution of the cosmological parameters that is approximated by the relation $0.8\Omega_M - 0.6\Omega_\Lambda \approx -0.2 \pm 0.1$ in the region of interest ($\Omega_M \lesssim 1.5$). For a flat ($\Omega_M + \Omega_\Lambda = 1$) cosmology we find $\Omega_M^{\text{flat}} = 0.28^{+0.09}_{-0.08}$ (1σ statistical) $^{+0.05}_{-0.04}$ (identified systematics). The data are strongly inconsistent with a $\Lambda = 0$ flat cosmology, the simplest inflationary universe model. An open, $\Lambda = 0$ cosmology also does not fit the data well: the data indicate that the cosmological constant is nonzero and positive, with a confidence of $P(\Lambda > 0) = 99\%$, including



Dark Energy and the Nobel Prize



PRESSMEDDELANDE

Press release

4 October 2011

The Nobel Prize in Physics 2011

The Royal Swedish Academy of Sciences has decided to award the Nobel Prize in Physics for 2011 with one half to

Saul Perlmutter

The Supernova Cosmology Project

Lawrence Berkeley National Laboratory and University of California,
Berkeley, CA, USA

and the other half to

Brian P. Schmidt

and

The High-z Supernova Search Team

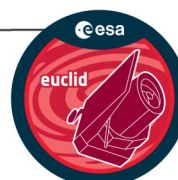
Australian National University,
Weston Creek, Australia

Adam G. Riess

The High-z Supernova Search Team

Johns Hopkins University and Space Telescope Science Institute,
Baltimore, MD, USA

"for the discovery of the accelerating expansion of the Universe through observations of distant supernovae".



How the Universe evolves



High redshift ($z=1000$) Tiny Density Fluctuations
CMB $\Delta T / T \sim 10^{-5}$



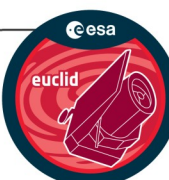
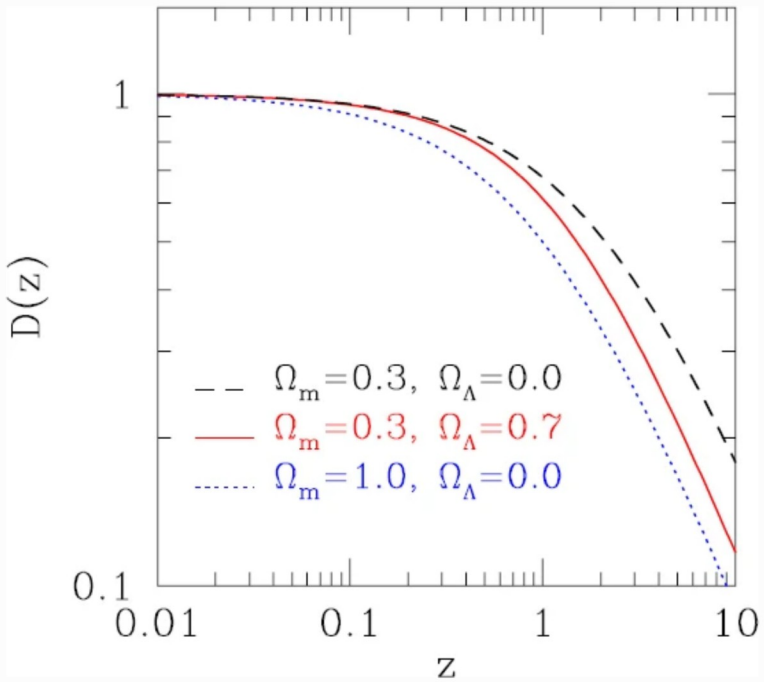
GRAVITY

Low redshift ($z < 0.5$)
Large Density Fluctuations
Clusters, Groups, Isolated Galaxies, Voids

The growth of these fluctuations depends on how strong gravity is: how much mass there is and what is the law of gravity

We measure these fluctuations using the Galaxy correlation function

Linear growth of density fluctuations
Lahav & Suto 2004



How to measure it: two probes

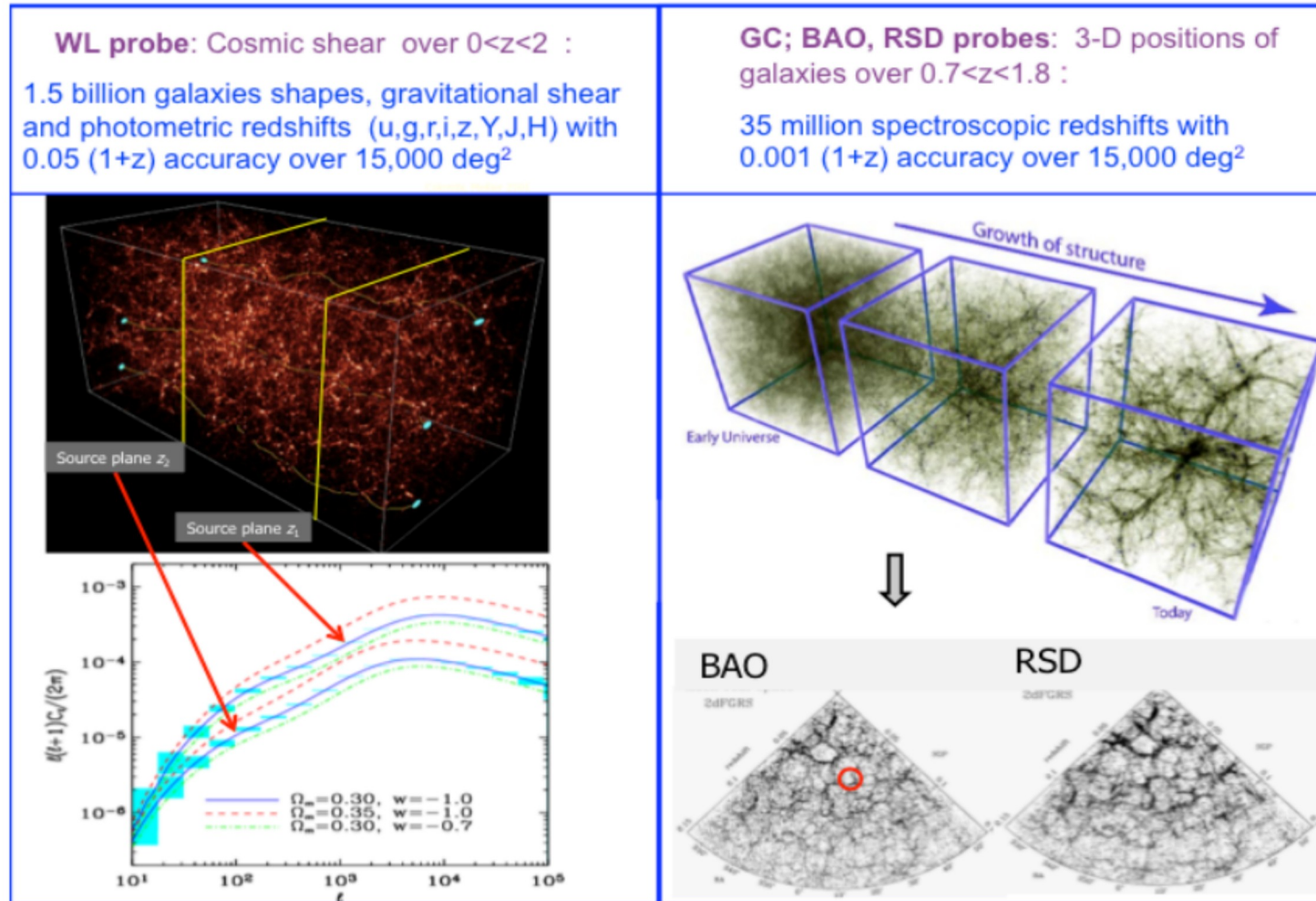


Illustration of the primary probes of the Euclid mission. Right: Galaxy Clustering (GC), including Baryon acoustic oscillations, (BAO), Redshift Space Distortion (RSD). Left: Weak Lensing (WL)- Courtesy Euclid Consortium/Science Working Group.

Weak Lensing

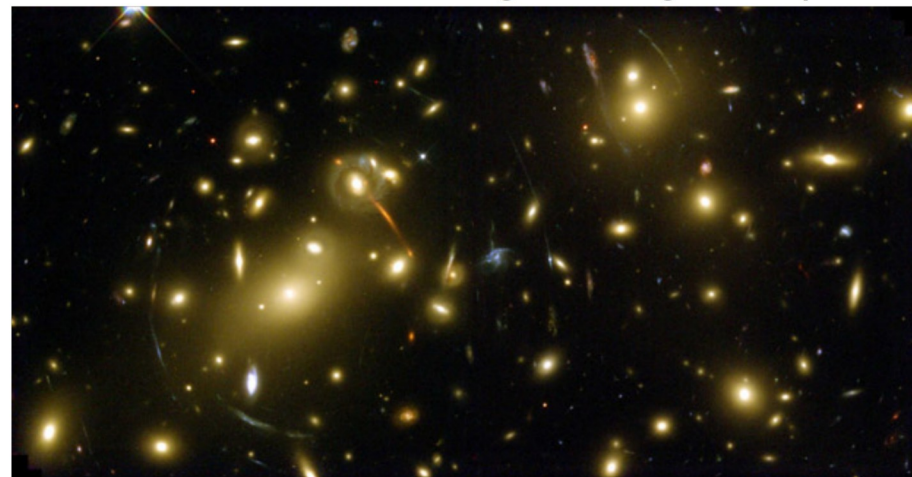
- It's the poor relative of the spectacular effect seen in intermediate distance clusters of galaxies (Strong Lensing)
- Can only be measured statistically, using large samples of galaxies

PRO: it's sensitive to the TOTAL amount of matter

CON: low resolution in redshift

CON: tiny effect; measurement dominated by PSF systematics;
unknown role of intrinsic alignements

Strong Lensing Example



Galaxy Clustering

- It provides a number of different probes that can be used to monitor the evolution of the large-scale matter distribution in the Universe
- Most important are: Barionic Acoustic Oscillations (BAO) and Redshift Space Distortions

CON: can only trace visible, baryonic matter

CON: need to determine unknown relationship between visible and total matter

PRO: different probes can be used for consistency checks

PRO: high redshift resolution

Kaiser 1987

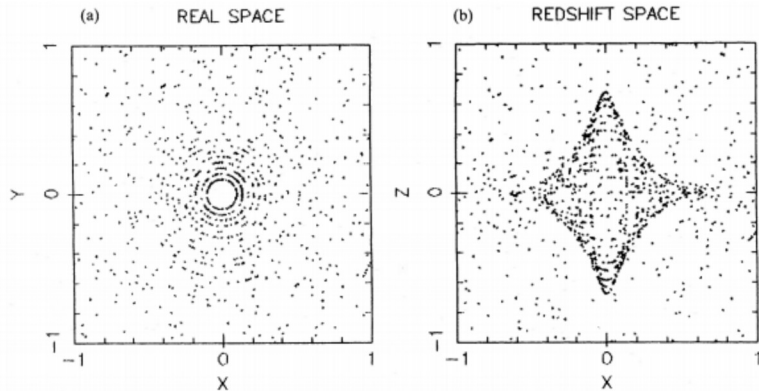


Figure 5. Spherical cluster with power law density profile in r -space (a) and as it appears in redshift space (b). The points shown are those which lie in a thin equatorial slice through the cluster centre. Points in the central virialized portion have been omitted. Innermost points are falling into the cluster for the first time. The sampling density and separation between shells are such that individual shells can still be seen in s -space (z -coordinate is the redshift direction). The density contrast profile is $\Delta(r) = (r/1.4)^{-1.75}$. A caustic surface has resulted in s -space which, in three dimensions, has the form of two trumpet horns glued face to face. The caustic surface extends to the turnaround radius which lies at roughly twice the central 1D velocity dispersion, or about $20h^{-1}$ Mpc for a cluster like Coma.

How the Euclid Mission was born



Noname manuscript No.
(will be inserted by the editor)

The Dark UNiverse Explorer (DUNE): Proposal to ESA's Cosmic Vision

A. Refregier and the DUNE collaboration*

* **Co-investigators:** A. Refregier (PI, CEA Saclay) · M. Dousspis (IAS Orsay) · Y. Mellier (IAP Paris) · B. Milliard (LAM Marseille) · P. Schneider (U. Bonn) · H.-W. Rix (MPIA) · R. Bender (MPE Garching) · F. Eisenhauer (MPE Garching) · R. Scaramella (INAF-OARM) · L. Moscardini (U. Bologna) · L. Amendola (INAF-OARM) · F. Pasian (INAF-OATS) · F.-J. Castander (ICE, Barcelona) · M. Martinez (IFAE, Barcelona) · R. Miquel (IFAE Barcelona) · E. Sanchez (CIEMAT Madrid) · S. Lilly (ETH Zurich) · G. Meylan (EPFL-UniGE) · M. Carollo (ETH Zurich) · F. Wildi (EPFL-UniGE) · J. Peacock (IfA Edinburgh) · S. Bridle (UCL London) · M. Cropper (MSSL) · A. Taylor (IfA Edinburgh) · J. Rhodes (JPL) · J. Hong (JPL) · J. Booth (JPL) · S. Kahn (U. Stanford) · **WG coordinators:** A. Amara (CEA Saclay) · N. Aghanim (IAS Orsay) · J. Weller (UCL) · M. Bartelmann (ZAH Heidelberg) · L. Moustakas (JPL) · R. Somerville (MPIA) · E. Grebel (ZAH Heidelberg) · J.-P. Beaulieu (IAP Paris) · M. Della Valle (Arcetri) · I. Hook (U. Oxford) · O. Lahav (UCL London) · A. Fontana (Roma) · D. Bederde (CEA Saclay) · **Science:** F. Abdalla (UCL) · R. Angulo (Durham) · V. Antonuccio (Catane) · C. Baccigalupi (SISSA) · D. Bacon (U. Edinburgh) · M. Banerji (UCL) · E. Bell (MPIA) · N. Benitez (Madrid) · S. Bonometto (Milano) · F. Bournaud (CEA Saclay) · P. Capak (Caltech) · F. Casoli (IAS Orsay) · L. Colombo (Milano) · A. Cooray (UC Irvine) · F. Courbin (EPFL) · E. Cypriano (UCL) · H. Dahle (Oslo) · R. Ellis (Caltech) · T. Erben (Bonn) · P.

How the Euclid Mission was born



Noname manuscript No.
(will be inserted by the editor)

04.4433v1 [astro-ph] 28 Apr 2008

SPACE: the SPectroscopic All-sky Cosmic Explorer

2

- A. Cimatti¹ · M. Robberto² · C. Baugh³ · S. V. W. Beckwith² · R. Content⁴ · E. Daddi⁵ · G. De Lucia⁶ · B. Garilli⁷ · L. Guzzo⁸ · G. Kauffmann⁶ · M. Lehnert⁹ · D. Maccagni⁷ · A. Martínez-Sansigre¹⁰ · F. Pasian¹¹ · I. N. Reid² · P. Rosati¹² · R. Salvaterra¹³ · M. Stiavelli² · Y. Wang¹⁴ · M. Zapatero Osorio¹⁵
- M. Balcells¹⁵ · M. Bersanelli¹³ · F. Bertoldi¹⁶ · J. Blaizot⁶ · D. Bottini⁷ · R. Bower³ · A. Bulgarelli¹⁷ · A. Burgasser¹⁸ · C. Burigana¹⁷ · R. C. Butler¹⁷ · S. Casertano² · B. Ciardi⁶ · M. Cirasuolo¹⁹ · M. Clampin²⁰ · S. Cole³ · A. Comastri²¹ · S. Cristiani¹¹ · J.-G. Cuby²² · F. Cuttaia¹⁷ · A. De Rosa¹⁷ · A. Diaz Sanchez²³ · M. Di Capua²⁴ · J. Dunlop^{19,25} · X. Fan²⁶ · A. Ferrara²⁷ · F. Finelli¹⁷ · A. Franceschini²⁸ · M. Franx²⁹ · P. Franzetti⁷ · C. Frenk³ · Jonathan P. Gardner²⁰ · F. Gianotti¹⁷ · R. Grange²² · C. Gruppioni²¹ · A. Gruppuso¹⁷ · F. Hammer⁹ · L. Pozzetti²¹ · J. Rayner⁴¹ · R. Rebolo¹⁵ · A. Renzini⁴² · H. Röttgering²⁹ · E. Schinnerer¹⁰ · M. Scodéggi⁷ · M. Saisse²² · T. Shanks³ · A. Shapley⁴³ · R. Sharples⁴ · H. Shea⁴⁴ · J. Silk⁴⁵ · I. Smail³ · P. Spanó⁸ · J. Steinacker¹⁰ · L. Stringhetti¹⁷ · A. Szalay⁴⁶ · L. Tresse²² · M. Trifoglio¹⁷ · M. Urry⁴⁷ · L. Valenziano¹⁷ · F. Villa¹⁷ · I. Villo Perez²³ · F. Walter¹⁰ · M. Ward³ · R. White² · S. White⁶ · E. Wright⁴⁸ · R. Wyse⁴⁶ · G. Zamorani²¹ · A. Zacchei¹¹ · W.W. Zeilinger⁴⁹ · F. Zerbi⁸

Received: November 21, 2007 / Accepted: 10 Apr, 2008

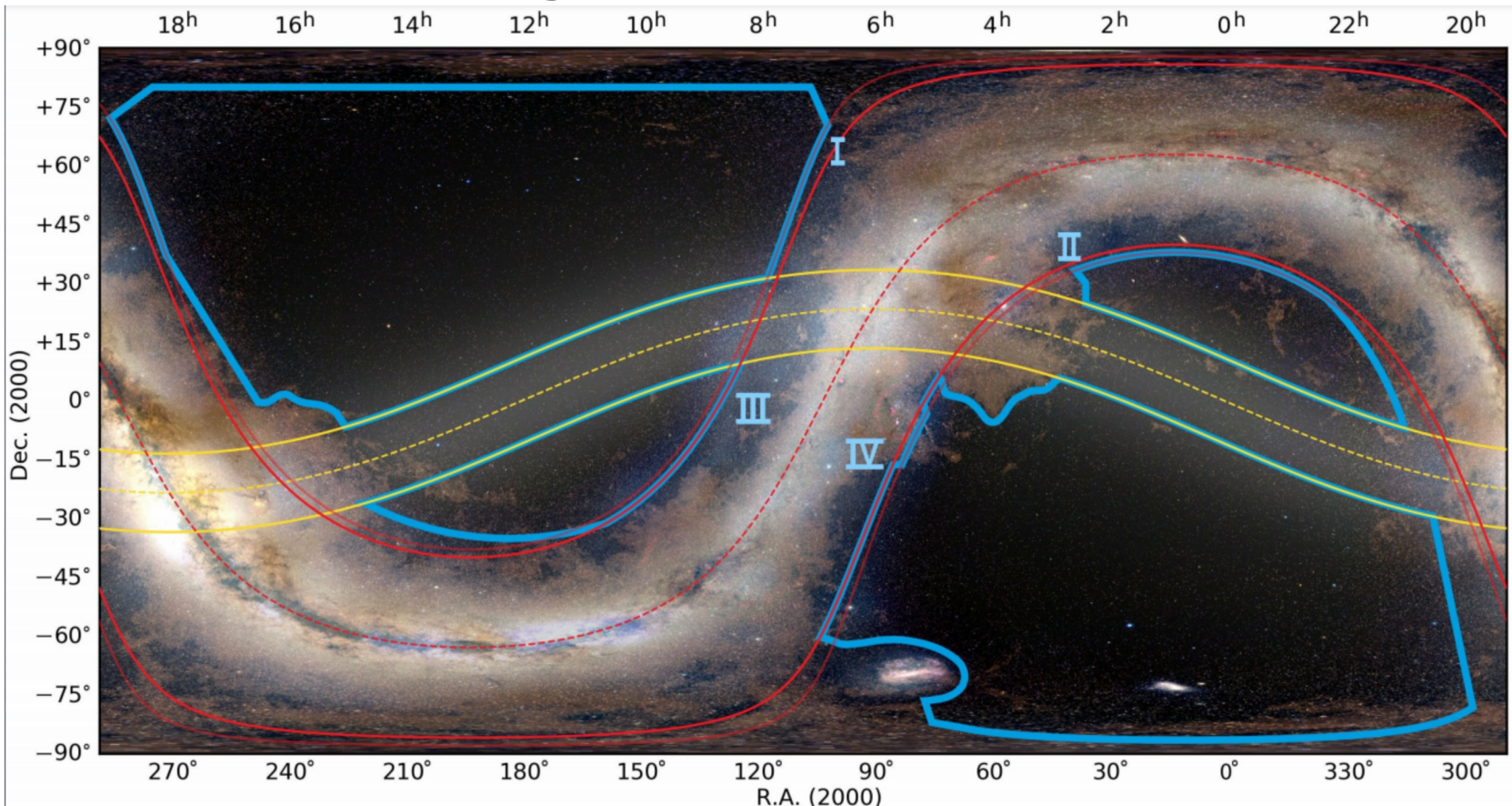
The marriage results (October 2011)

Euclid Mission Summary



Main Scientific Objectives							
Understand the nature of Dark Energy and Dark Matter by:							
<ul style="list-style-type: none"> Reach a dark energy $FoM > 400$ using only weak lensing and galaxy clustering; this roughly corresponds to 1 sigma errors on w_p and w_a of 0.02 and 0.1, respectively. Measure γ, the exponent of the growth factor, with a 1 sigma precision of < 0.02, sufficient to distinguish General Relativity and a wide range of modified-gravity theories Test the Cold Dark Matter paradigm for hierarchical structure formation, and measure the sum of the neutrino masses with a 1 sigma precision better than 0.03eV. Constrain n_s, the spectral index of primordial power spectrum, to percent accuracy when combined with Planck, and to probe inflation models by measuring the non-Gaussianity of initial conditions parameterised by f_{NL} to a 1 sigma precision of ~ 2. 							
SURVEYS							
Wide Survey	Area (deg ²) 15,000 (required) 20,000 (goal)	Description Step and stare with 4 dither pointings per step.					
Deep Survey	40	In at least 2 patches of $> 10 \text{ deg}^2$ 2 magnitudes deeper than wide survey					
PAYOUT							
Telescope	1.2 m Korsch, 3 mirror anastigmat, $f=24.5 \text{ m}$						
Instrument	VIS	NISP					
Field-of-View	$0.787 \times 0.709 \text{ deg}^2$	$0.763 \times 0.722 \text{ deg}^2$					
Capability	Visual Imaging	NIR Imaging Photometry		NIR Spectroscopy			
Wavelength range	550– 900 nm	Y (920-1146nm), J (1146-1372 nm)	H (1372-2000nm)	1100-2000 nm			
Sensitivity	24.5 mag 10σ extended source	24 mag 5σ point source	24 mag 5σ point source	$3 \cdot 10^{-16} \text{ erg cm}^{-2} \text{ s}^{-1}$ 3.5σ unresolved line flux			
Detector Technology	36 arrays $4k \times 4k$ CCD	16 arrays $2k \times 2k$ NIR sensitive HgCdTe detectors					
Pixel Size	0.1 arcsec	0.3 arcsec		0.3 arcsec			
Spectral resolution	$R=250$						
SPACECRAFT							
Launcher	Soyuz ST-2.1 B from Kourou						
Orbit	Large Sun-Earth Lagrange point 2 (SEL2), free insertion orbit						
Pointing	25 mas relative pointing error over one dither duration						

The Euclid Survey Plan



The Euclid Wide Survey based on ecliptic&galactic latitude thresholds + upper limits on stellar density & extinction (Gaia/Planck)

- Euclid Wide Survey region of interest : 17 Kdeg.² compliant with a 15 Kdeg.² survey
- Ecliptic plane [zodiacal light background] : +/- 10 deg. ecliptic latitude exclusion zone
- Galactic plane [stellar contamination] : +/- 23&25 deg. galactic latitude exclusion zone

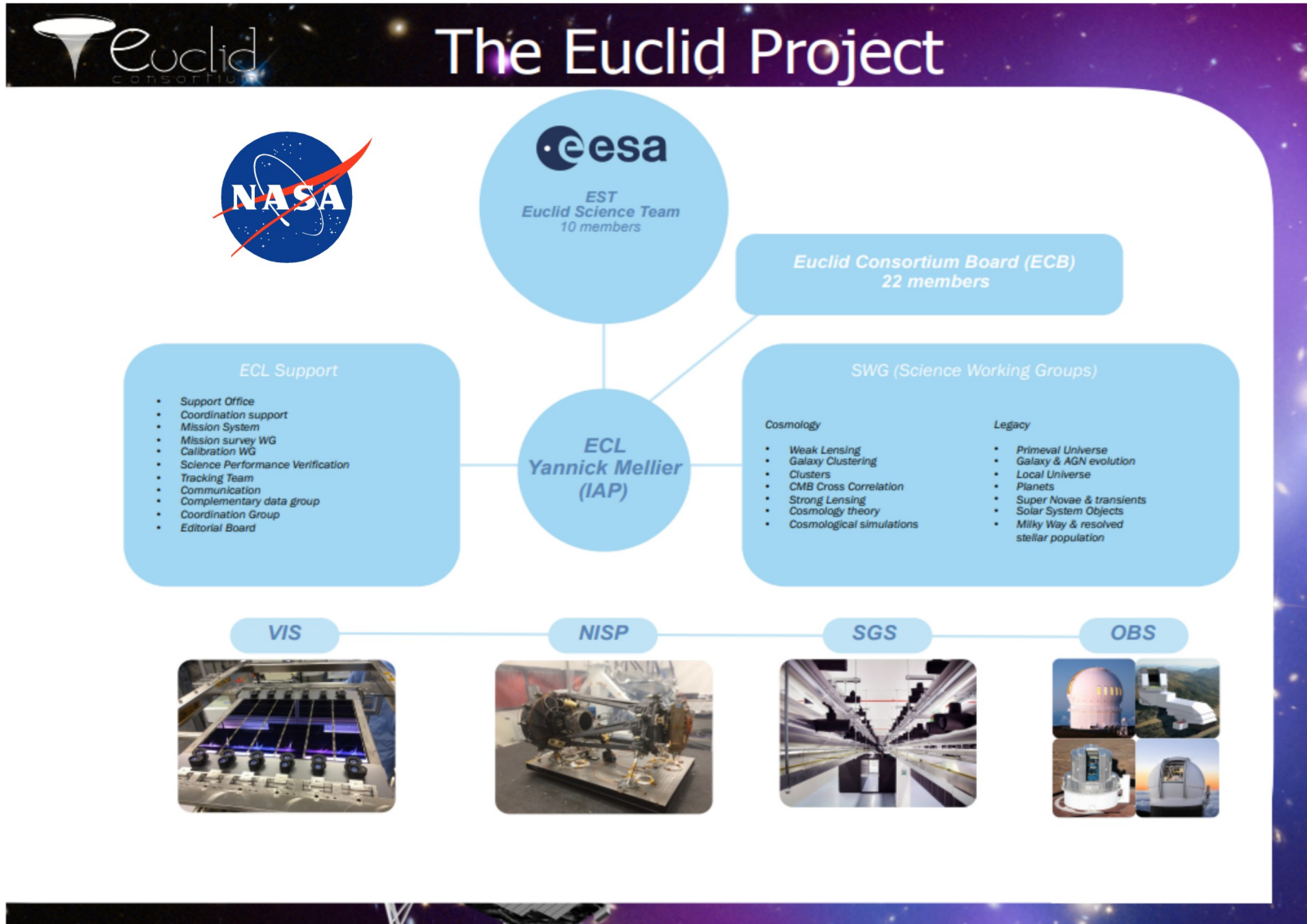


Background image: Euclid Consortium / A. Mellinger / Planck Collaboration

Last updated Euclid ROI: ~ 17,400 square degrees



The Euclid Consortium



Marco Scodéglio – The Status of the Euclid Mission - 24/02/2021



VIS and Weak Lensing

- Simple imaging camera, with no moving parts for maximum stability
- One large bandpass filter (covering r+i+z)
- 36 4k x 4k CCDs arranged in a 6 x 6 mosaic
- Pixel size 0.1 arcsec
- Built in UK, by UCL-Mullard Space Science Laboratory (with a small but significant Italian contribution)

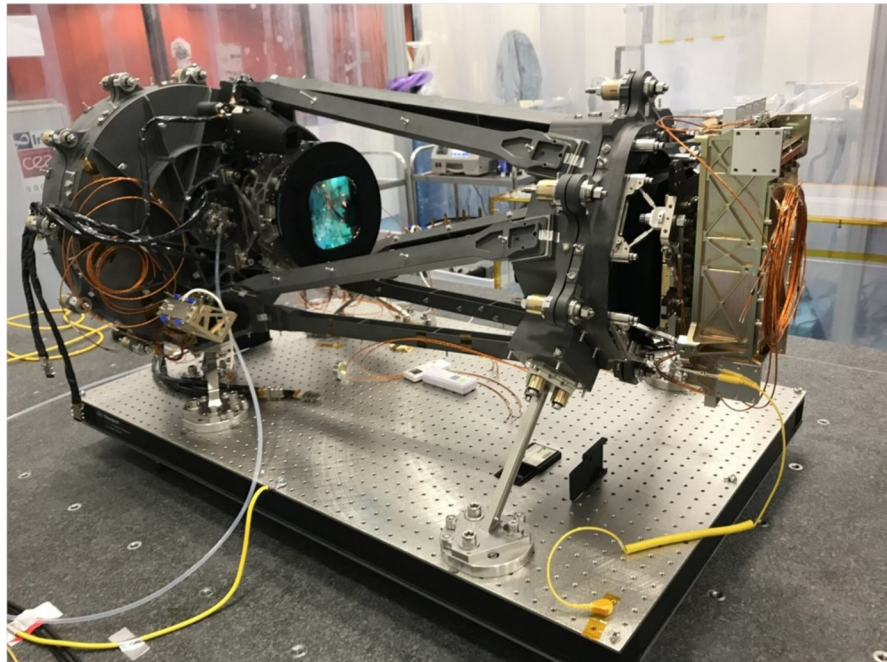
The VIS focal plane assembly



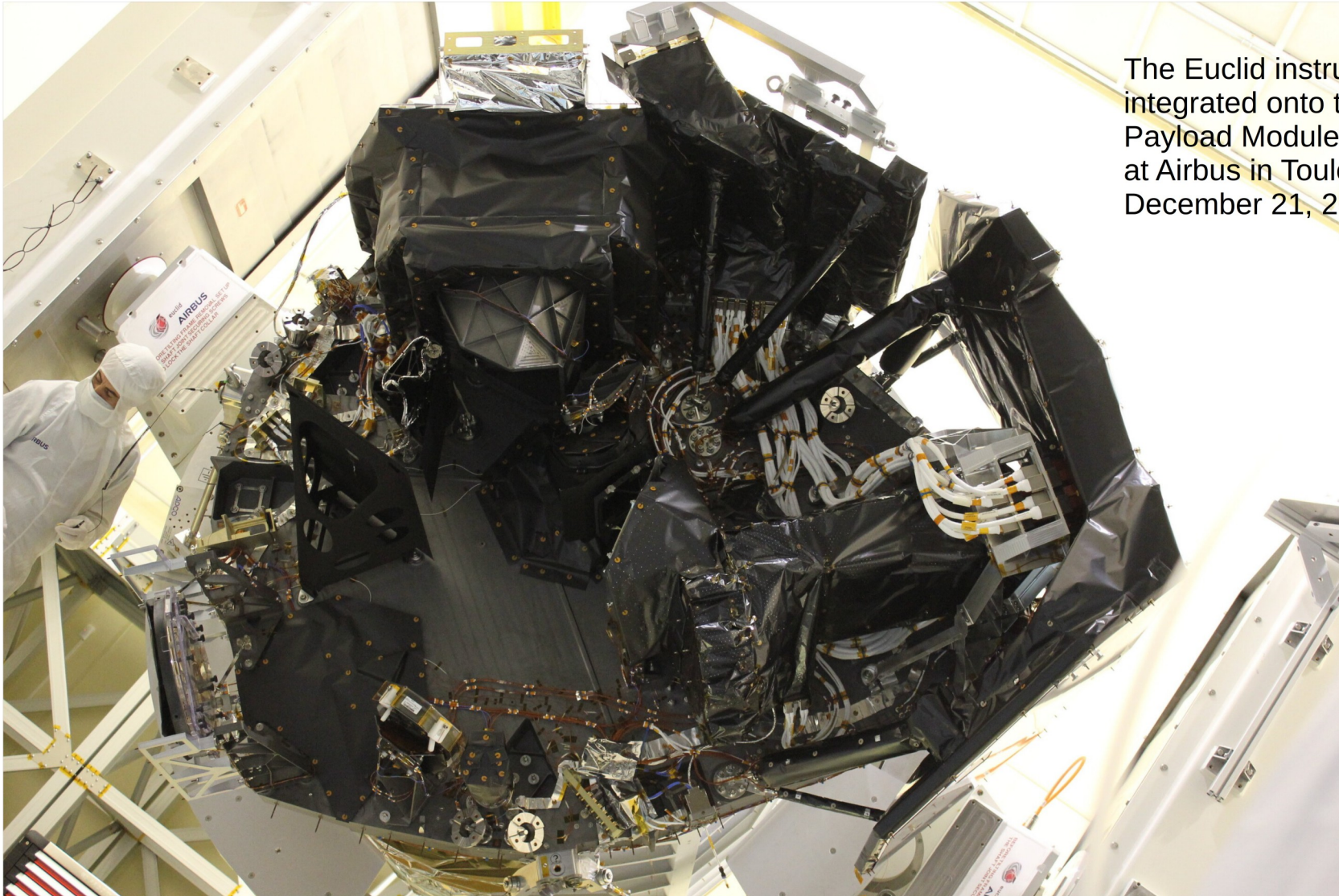
NISP and Galaxy Clustering

- More complex instrument, providing imaging and slitless spectroscopy capabilities
- 3 imaging bands (YJH), 2 grism bandpasses (920-1250 and 1250-1850 nm)
- 16 2k x 2k IR detectors, arranged in a 4 x 4 mosaic
- Pixel size 0.3 arcsec
- Built in France, with significant Italian contributions

The NISP instrument undergoing some testing



All together now

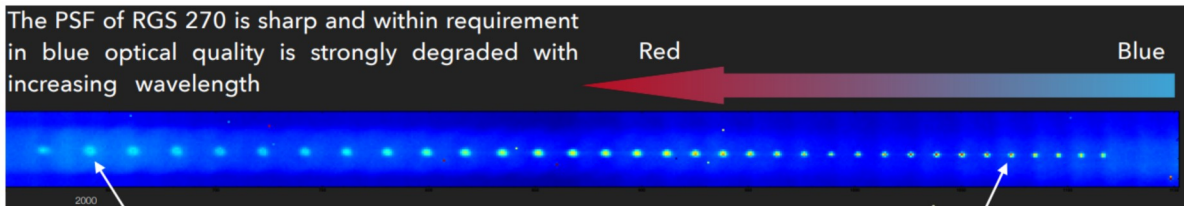


The Euclid instruments
integrated onto the
Payload Module
at Airbus in Toulouse
December 21, 2020

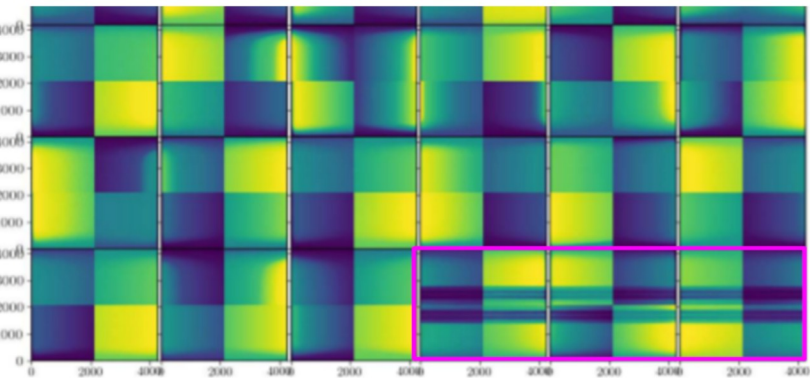
A few bumps on the road

- The Refregier accident
- The NISP detectors readout electronics problem (Spring 2017)
- The NISP grisms problem (Jan 2020)

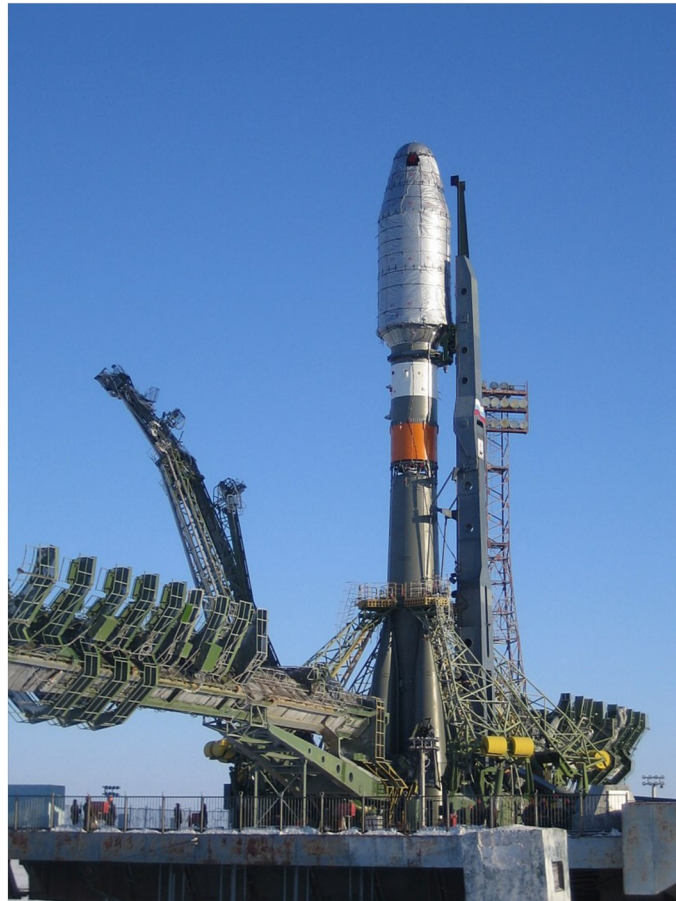
The PSF of RGS 270 is sharp and within requirement in blue optical quality is strongly degraded with increasing wavelength



- The VIS detectors readout electronics problem (Dec 2020)



- The use of the Soyuz ST-2.1B as launcher



Science Working Groups



Euclid Primary Science

Galaxy Clustering



L. Guzzo

Weak Lensing

Other Cosmology SWGs

Clusters of Galaxies



L. Moscardini

CMB Cross-correlation



C. Bacigalupi

Strong Lensing



M. Meneghetti

Cosmology Theory



*L. Amendola

Cosmology Simulations

Euclid Legacy Science

Primordial Universe

Galaxy & AGN Evolution

Local Universe



A. Cimatti



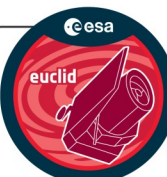
L. Hunt

Planets

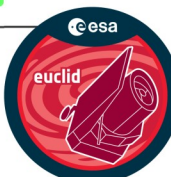
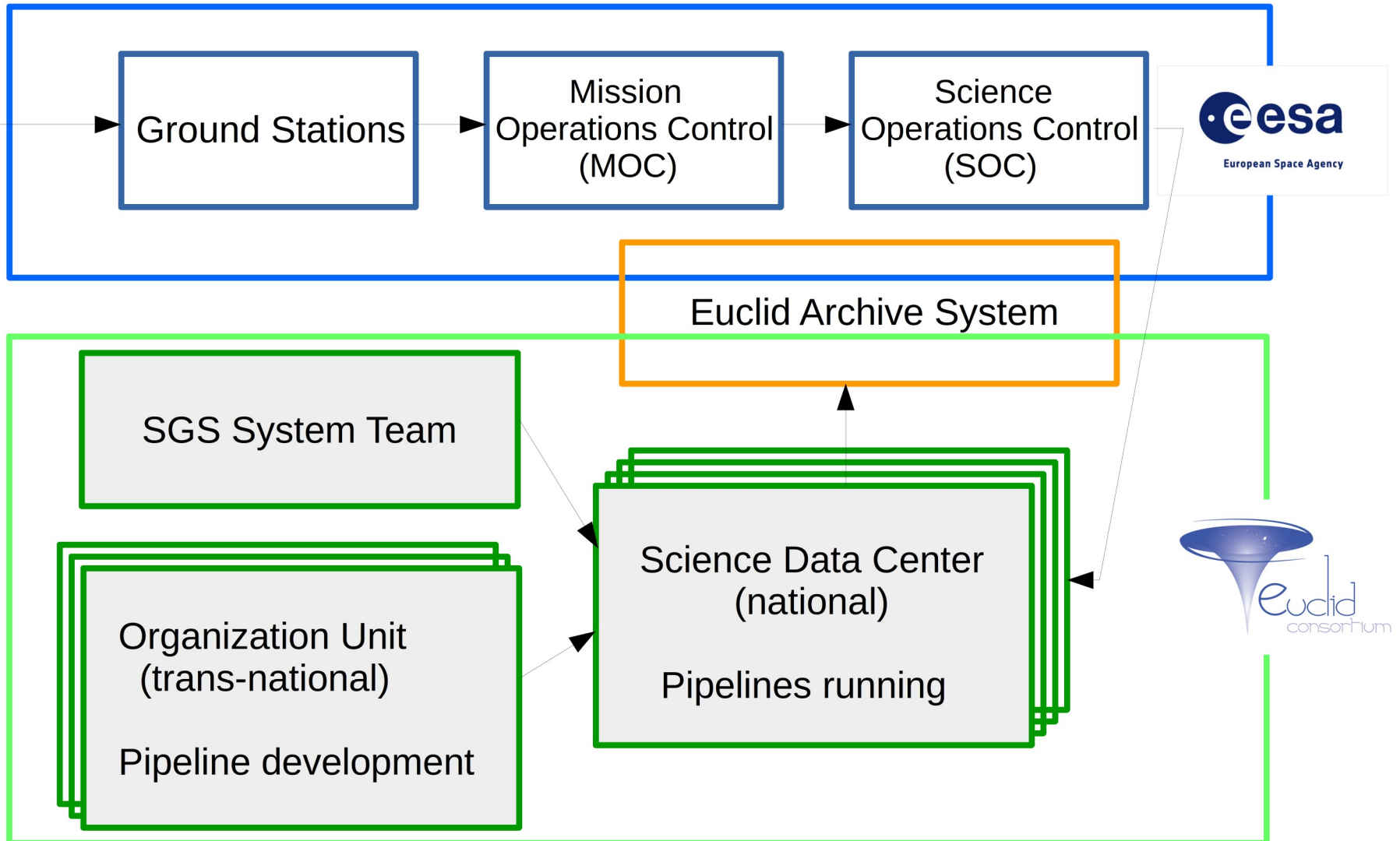
Supernovae & trans.

Solar System Objects

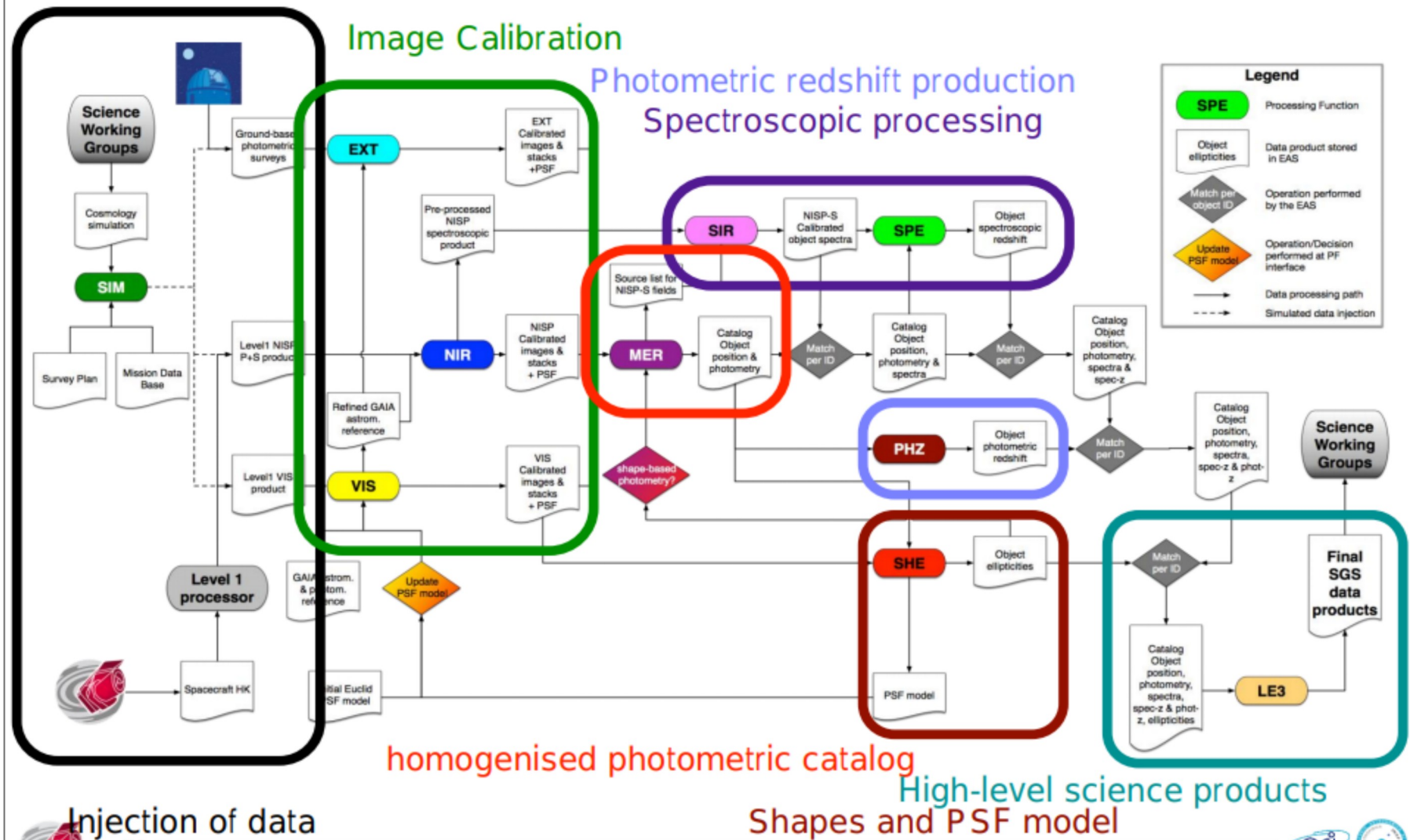
MW and resolved stellar pop.



The Science Ground Segment



The Science Ground Segment



What do we do in Italy

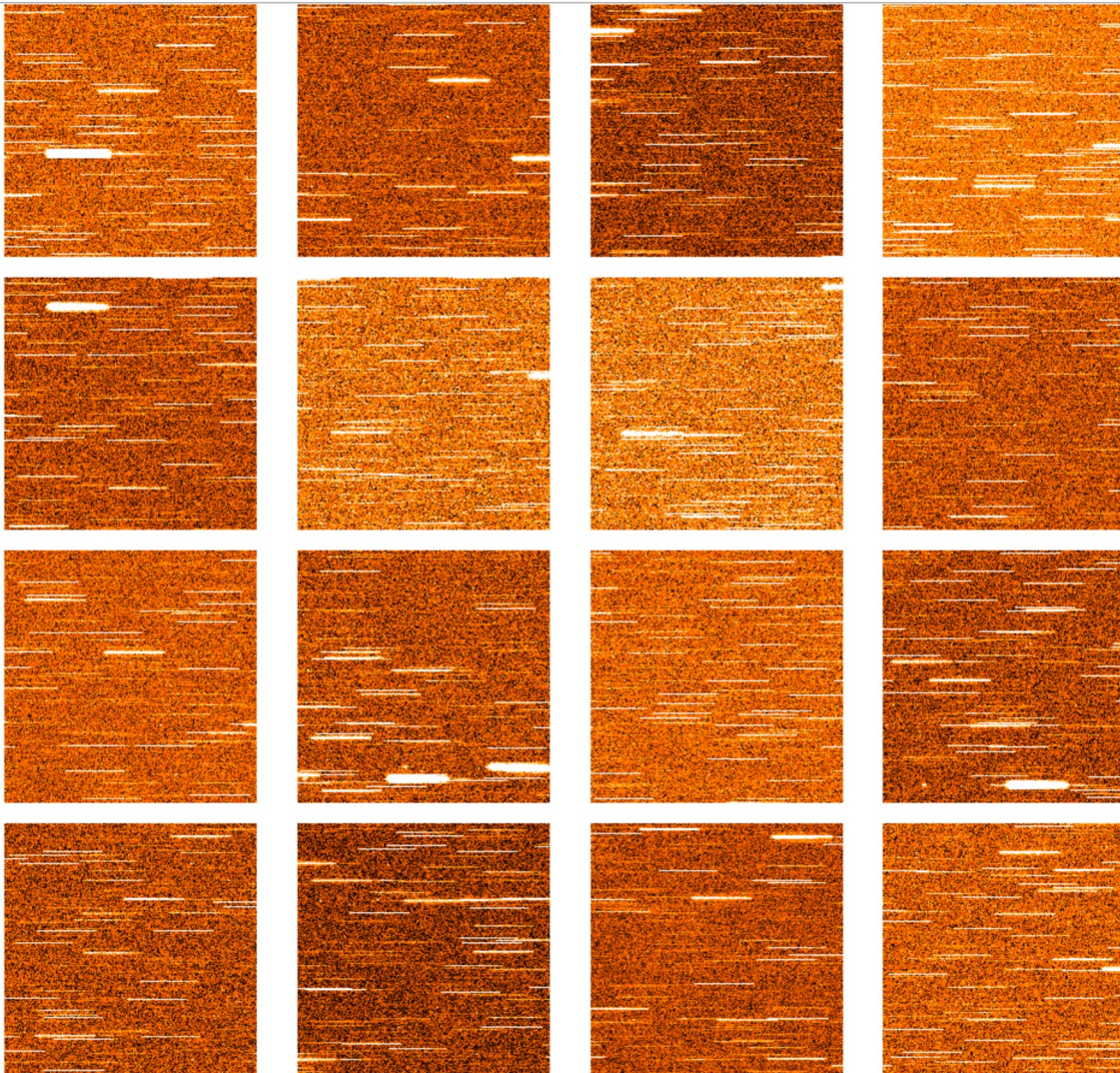
- Galaxy Clustering (Milano, Bologna, Roma, Trieste, Genova, Padova)
- Galaxy Clusters (Bologna, Milano, Trieste)
- CMB-X (Trieste, Padova, Milano)
- Galaxy & AGN Evolution (everywhere)
- Lensing (Roma, Bologna)

- SGS-Project Office + SDC-IT (Trieste)
- OU-NIR (Roma) + OU-MER (Roma) + OU-SIR (Milano, Genova)
- OU-LE3 (Roma, Bologna, Trieste, Milano)
- Participations to OU-SPE, OU-PHZ
- VIS and NISP Instrument Development Teams

What do we do in Milano

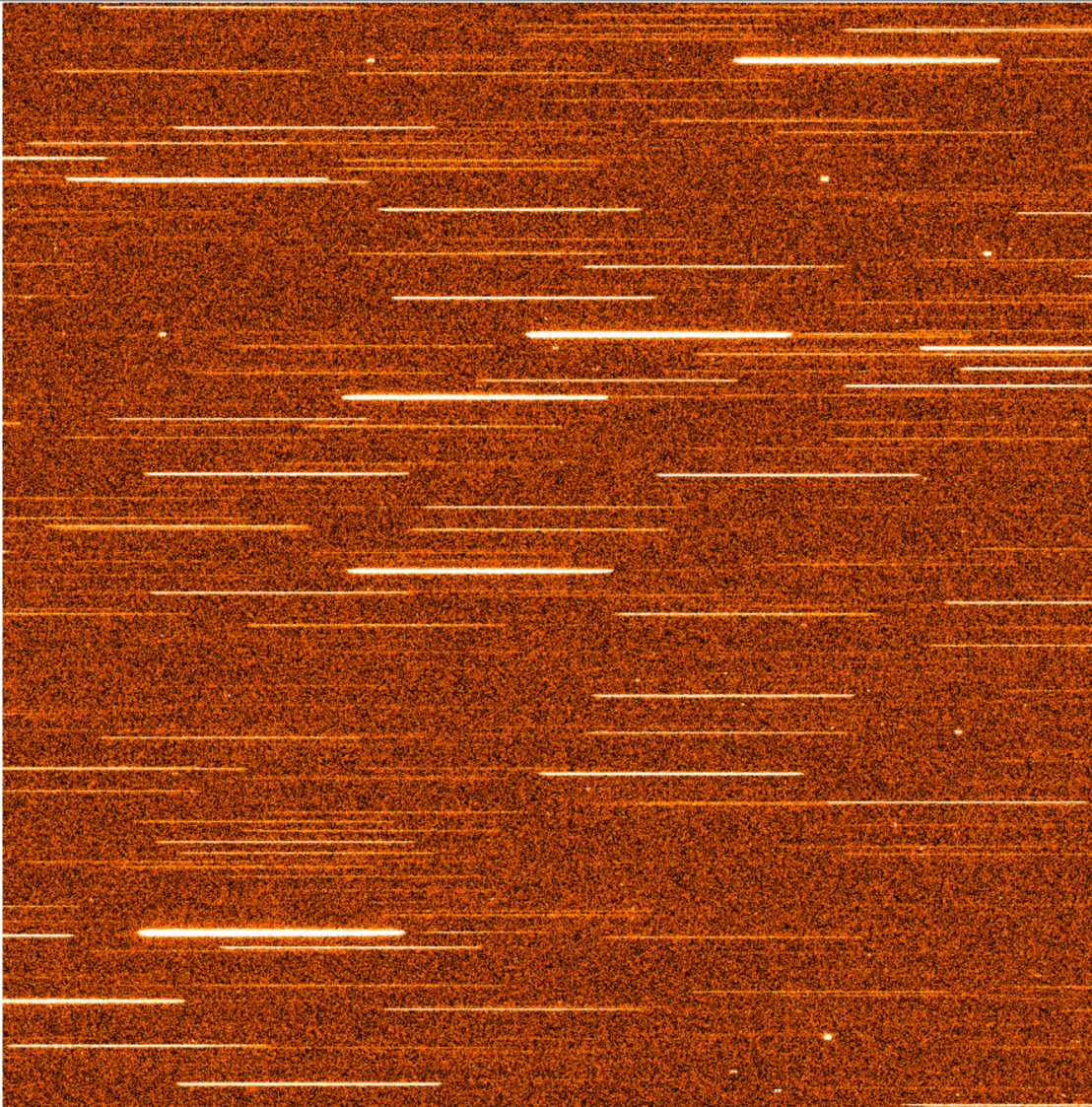
- Galaxy Clustering (Guzzo, Archidiacono, Granett, Carbone)
- Galaxy Clusters (Andreon, Iovino)
- **Simulations, CMB-X, Neutrinos, Gravitational Waves (Carbone)**
- Galaxy evolution (Mancini, Scodeggio, Granett, Garilli)
- **OU-SIR, spectroscopic pipeline (Scodeggio, Fumana, Mancini, Maino, Garilli, Franzetti)**
- OU-LE3, selection functions (Granett)

The spectroscopic data



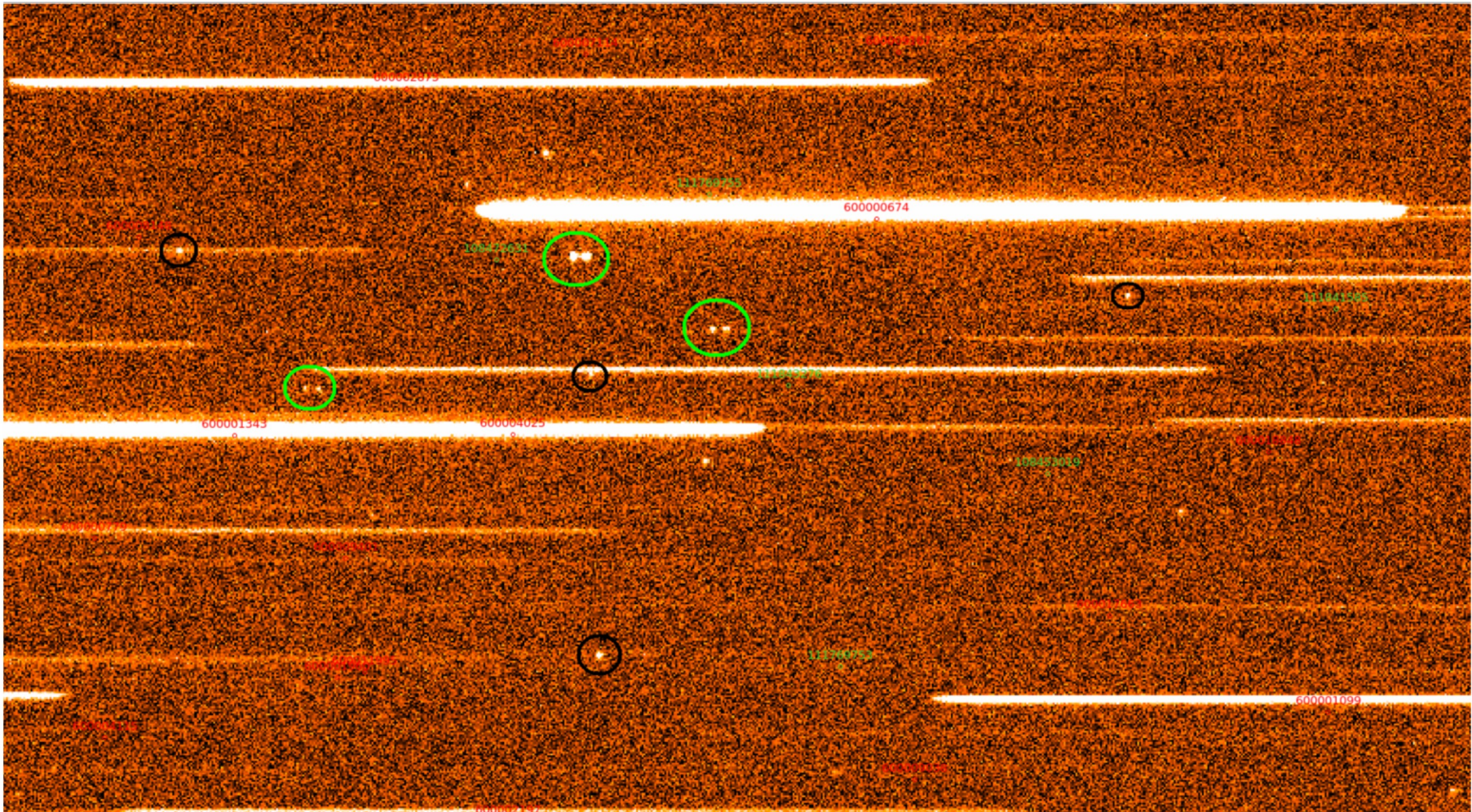
Simulated full NISP
spectroscopic
exposure

The spectroscopic data



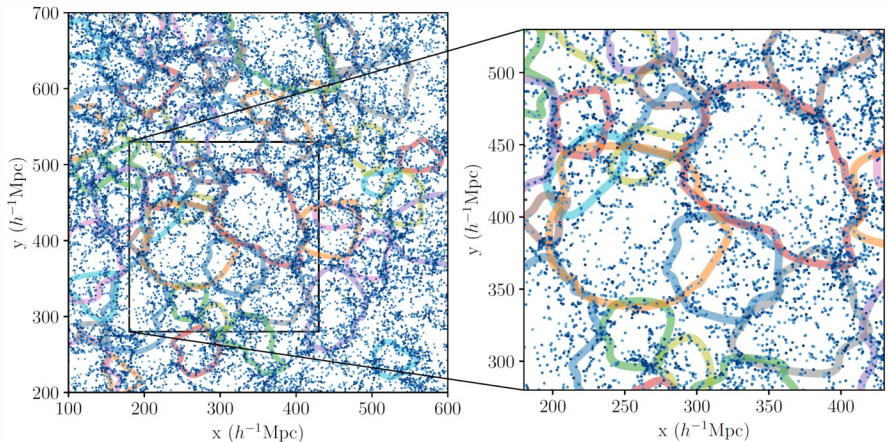
Simulated single NISP
detector spectroscopic
exposure

The spectroscopic data



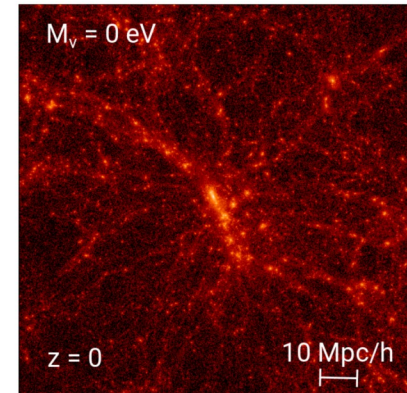
Zoom-in into a simulated NISP spectroscopic exposure (green circles = zeroth-order spectra; black circles = Halpha emission lines)

The cosmological simulations

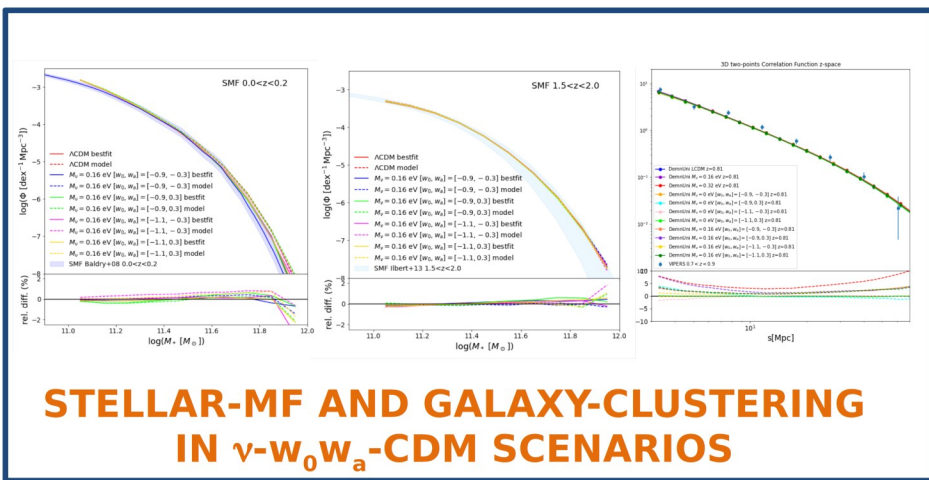


Voids

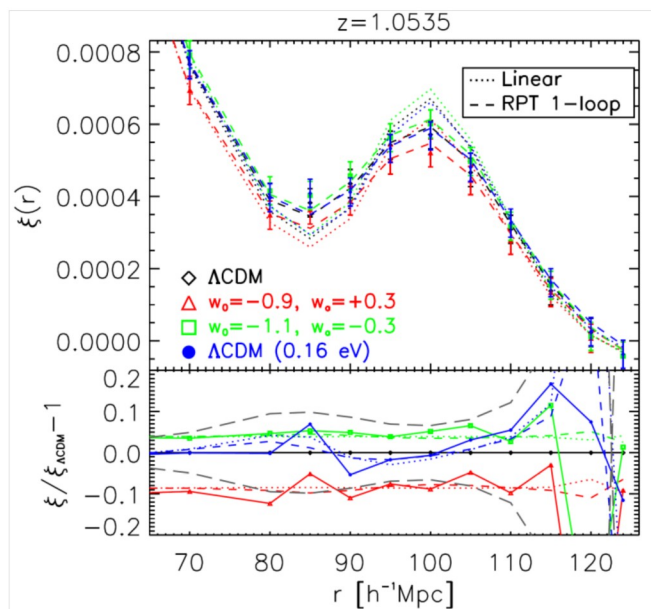
Clusters



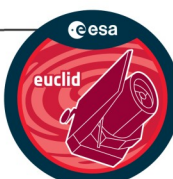
DEMNUni simulations



**STELLAR-MF AND GALAXY-CLUSTERING
IN ν - w_0w_a -CDM SCENARIOS**



BAOs in different scenarios



The near-future timeline

- April-May 2021: a decision about VIS problems
- May-June 2021: PLM testing (56 days of testing)
- Sept 2022 (as of today....): launch
- First month: Commissioning
- Second & Third month: Performance and Verification
- After 3 months, T0: Early Survey Operations
- T0 + 14 months: the Q1 data release, a quick and dirty [and limited] data release to show the potential of Euclid data
- T0 + 2 years: the first real Euclid data release - the data taken during the first year of the survey

That's all Folks!

Isberg®